Single and double electron capture in N^{5+}+H_2 collisions at low impact energies.

L. F. Errea, L. Fernández, A. Macías,* L. Méndez, I. Rabadán, and A. Riera

Laboratorio Asociado al CIEMAT de Física Atómica y Molecular en Plasmas de Fusión.

Departamento de Química, Universidad Autónoma de Madrid, Madrid-28049, Spain

Abstract

We present *ab initio* calculations of cross sections for single and autoionizing double electron capture in collisions of N^{5+} with H_2 , for impact energies between 0.2 and 10 keV/amu. Calculations have been carried out by means of a close-coupling molecular treatment using the sudden approximation for rotation and vibration of the diatomic molecules. Since the molecular states involved are infinitely excited, a configuration interaction method, with a block-diagonalization procedure, has been employed to evaluate potential energy surfaces and dynamical couplings.

*Instituto de Estructura de la Materia, CSIC, Serrano 123, Madrid-28006, Spain

I. INTRODUCTION

Electron capture processes in ion-molecule collisions are important reactions in the interaction of solar wind with cometary and planetary atmospheres (e.g. [1]) and fusion plasmas (e.g. [2]). In particular, N^{5+} + H_2 collisions have been studied in both experimental and theoretical works. Photon emission spectroscopy [3, 4] and translational energy spectroscopy [5] experiments have been carried out, and, as a general conclusion of these works, the most important processes at impact energies around 1keV/amu are the single electron capture (SEC):

$$N^{5+}(1s^2) + H_2(X^1\Sigma_g^+) \rightarrow N^{4+}(1s^2nl) + H_2^+(X^2\Sigma_g^+) \ , \tag{1}$$

with n=3,4, and the autoionizing double capture (ADC):

$$N^{5+}(1s^2) + H_2(X^1\Sigma_g^+) \rightarrow N^{3+}(1s^23l3l') + H^+ + H^+ \tag{2}$$

reactions. However, the cross sections for the ADC reaction (2) were not directly measured in ref. [5]; these were assumed to be equal to those for formation of $N^{4+}(1s^22l)$, which is the main product of the post-collision autoionization of N^{3+} after reaction (2).

Previous calculations [6, 7] for this system employed a one-electron approach, where the "active" electron moves in the effective potential created by the nuclei and the remaining electrons; i.e. the $N^{5+}$and H_2^+ cores. In particular, the pioneering work of ref. [6] employed a model potential formalism, and a similar treatment, with pseudopotentials, was used in [7]. While an effective potential description of the electron interaction with the N^{5+} core is a good approximation, a similar treatment for the interaction with the open-shell H_2^+ core is more questionable. In this respect, the calculation of ref. [8] for H^+ and Be^{4+} collisions with H_2 showed that a two-electron interpretation of the transition probabilities, not performed in refs. [6, 7], is required to evaluate single electron capture cross sections. Accordingly, a model potential treatment was applied to N^{5+} - H_2 in a previous calculation of our group [9] including the two-electron interpretation, and assuming that the two target electrons are equivalent (see [10–12]). This approach is usually known as independent electron approximation (e.g. in [13]) or independent particle model (IPM) (e.g. in [14]). An extension of the IPM was presented in [15], where the equivalent-electron interpretation was used to evaluate the Hamiltonian matrix elements rather than the transition probabilities, which allows to extend the range of applicability of the method to lower energies; this technique was applied

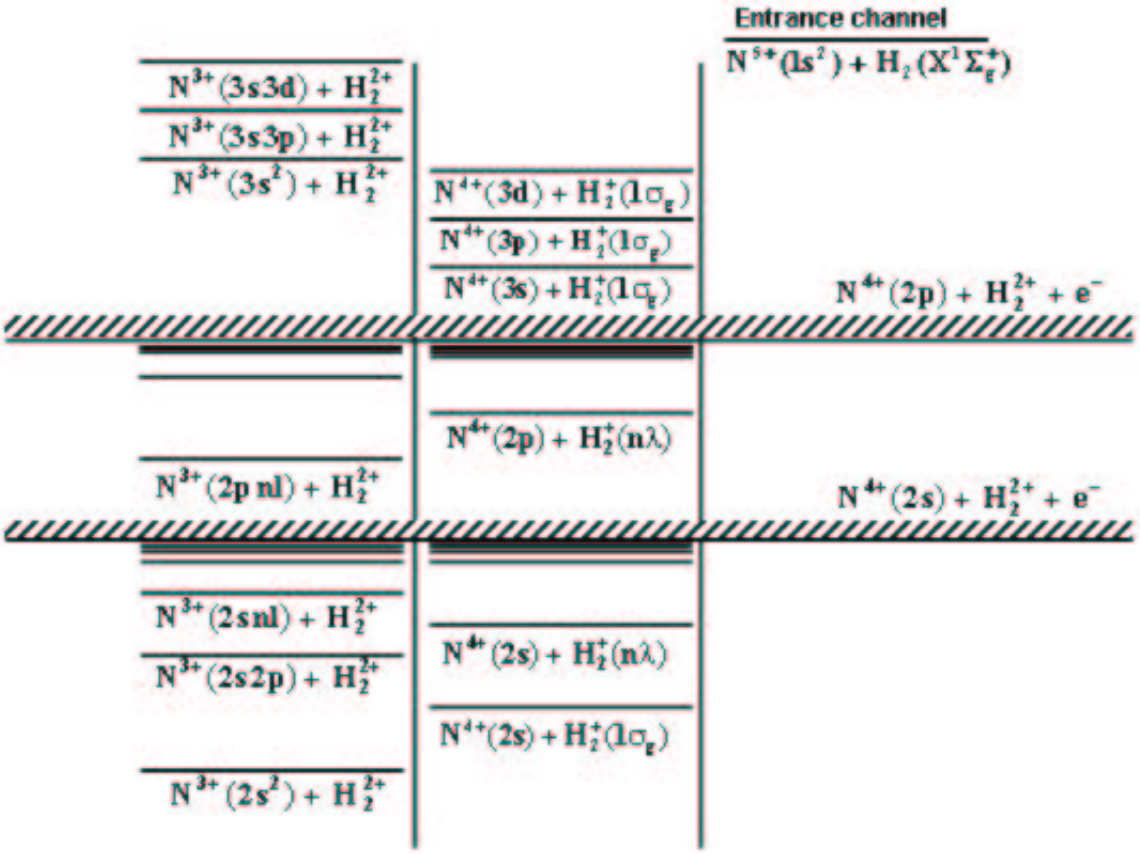

FIG. 1: Qualitative energy diagram of the asymptotic energies of the NH_2^{5+} quasimolecule.

to $N^{5+} + H_2$ collisions in ref. [16].

Although IPM treatments are appropriate to evaluate single electron capture cross sections, in general, they cannot accurately describe two-electron processes (see e.g. [17] and references therein), and therefore it is difficult to justify the application of the IPM when those processes are sizeable; this is the case of ion-H_2 collisions when double electron capture reactions are significant. However, for some particular collisions (see [15] and [18]), single and double electron capture take place through independent mechanisms, and the IPM yields accurate cross sections for single electron capture, although this can only be checked by comparison with all-electron calculations. The fact that only IPM calculations have been carried out for $N^{5+} + H_2$ collisions, even though, reactions (2) are expected to be competitive with (1), is mainly due to the difficulty of evaluating potential energy surfaces and dynamical couplings for the states of interest. The *ab initio* calculation of cross sections for reactions (1) and (2) is the main objective of the present paper.

An important difference between collisions of singly charged ions (see a recent example in ref. [19]) and those of multicharged ions with H_2 is the presence of infinitely excited states in the energy correlation diagram. In the particular case of N^{5+} + H_2 (see fig. 1), the energy of the the entrance channel N^{5+} $(1s^2)$+ $H_2(X^1\Sigma_g^+)$ lies above the four Rydberg series $N^{3+}(1s^22snl;\ 1s^22pnl)$ + H^+ + H^+ and $N^{4+}(1s^22s;1s^22p)$ + $H_2^+(n\lambda)$ (see fig. 1), and the main electron capture channels ($N^{4+}(1s^23l)$+$H_2^+(1\sigma_g)$) are also infinitely excited. Therefore, the molecular description of SEC involves transitions between states whose energies lie in the ionization continuum. To calculate the potential energy surfaces and dynamical couplings, we have employed, as in previous works for Be^{4+} and C^{4+} collisions with H_2 [20, 21] Block-Diagonalization (BD) techniques [22], where the molecular states are obtained by diagonalizing the matrix of the electronic Hamiltonian in a basis from which the configurations that asymptotically correlate to the states of the Rydberg series are excluded. The main difference between the asymptotic energies of fig.1 with respect those of the previously studied C^{4+} + H_2 and Be^{4+} + H_2 systems is that the energies of the ADC states $N^{3+}(1s^23l3l')$ lie below that of the entrance channel, which in principle allows for sizeable transitions to these states. In practice this means that the entrance channel of the collision is a high-lying root of the secular equation even though the BD procedure is applied.

The paper is organized as follows: The details of the molecular calculation and the dynamical method are presented in section II. Our results are shown in section III and the main conclusions are outlined in section IV. Atomic units are used unless otherwise indicated.

II. METHOD

A. Molecular calculations.

The potential energy surfaces and molecular wavefunctions of the NH_2^{5+} quasimolecule are expressed in terms of the following relative nuclear coordinates: The distance from the N^{7+} nucleus to the center of the H-H internuclear axis, R; the H-H internuclear distance, ρ, and the angle α between the vectors $\boldsymbol{R}$ and $\boldsymbol{\rho}$. Calling $\boldsymbol{r}$ the set of electronic coordinates, the molecular wavefunctions $\phi_j(\boldsymbol{r}; R, \rho, \alpha)$ are approximate eigenfunctions of the clamped-nuclei

Born-Oppenheimer electronic Hamiltonian, $H_{\rm elec}(\boldsymbol{r}; R, \rho, \alpha)$:

$$H_{\rm elec}(\boldsymbol{r}; R, \rho, \alpha) = \sum_{i=1}^{4} \left(-\frac{1}{2}\nabla_i^2 - \frac{7}{r_{i\rm N}} - \frac{1}{r_{i\rm H1}} - \frac{1}{r_{i\rm H2}} \right) + \sum_{i=1}^{4} \sum_{j<i}^{4} \frac{1}{r_{ij}} \tag{3}$$

where $r_{i\rm N}$, $r_{i\rm H1}$, $r_{i\rm H2}$ denote the distances from electron i to the three nuclei.

The molecular wavefunctions are obtained using a SCF-CI method by means of the program MELD [23], and employing a basis set of Gaussian type orbitals [33]. In a first step, a SCF calculation is performed to obtain the molecular orbitals (MO) of the NH_2^{7+} system. We have increased the molecular charge in this step to ensure that the unoccupied MOs (all except the ground MO) are good approximations to the orbitals of N^{4+} and H_2^+ in the limit $R \to \infty$.

A configuration interaction (CI) is then carried out. For singlet states the configurations have the form:

$$\psi_{kl} = \frac{1}{\sqrt{2}} \left[|| \; \xi_1 \overline{\xi_1} \xi_k \overline{\xi_l} \; || + || \; \xi_1 \overline{\xi_1} \xi_l \overline{\xi_k} \; || \right] \tag{4}$$

where ξ_j are MOs, $||\ \ ||$ denotes a Slater determinant, and where, to reduce the size of the CI space, we have applied the frozen core approximation in which the ground MO (ξ_1) is always doubly occupied. To evaluate the wavefunctions for the entrance channel and the main exit channels, whose potential energy surfaces are infinitely excited (see fig. 1), we have applied the block-diagonalization (BD) technique, originally proposed in [24], and applied to multicharged ion collisions with H_2 in refs. [20] and [21]. In the present case, we employ the method to remove the molecular states dissociating as $R \to \infty$ into those of the Rydberg series $N^{3+}(1s^2 2snl;\ 1s^2 2pnl) + H_2^{2+}$ and $N^{4+}(1s^2 2s; 1s^2 2p) + H_2^+(n\lambda)$, which is carried out by diagonalizing the matrix of the projected Hamiltonian $PH_{\rm elec}P$ with

$$P = 1 - \sum_{k=2}^{5} \sum_{l=2}^{N} |\psi_{kl}><\psi_{kl}| \,, \tag{5}$$

where N is the number of MOs. The matrix representation of $PH_{\rm elec}P$ is obtained by removing from the CI space those configurations in which the MOs ξ_k with $k = 2, 3, 4, 5$ are occupied, where the limits of these MOs, as $R \to \infty$ are, to an excellent approximation, the 2s and 2p orbitals of N^{4+}.

As a check of the accuracy of the calculation, we compare in table I the values of our molecular energies in the limit $R \to \infty$ with the spectroscopic values [25] for N^{4+} and N^{5+}ions, and with accurate calculations [26] for the autoionizing states of N^{3+}. Cuts of the

potential energy surfaces for $\alpha = 60^\circ$ are plotted in figs. 2, 3 and 4 for $\rho = 1.0$, 1.4 and 1.7 a.u., respectively. Except for α equal 0 or 90^0, the system has C_s symmetry. Since the entrance channel of the collision transforms like A', and only transitions to states of the same symmetry are allowed, we have only included states of A' symmetry in figs. 2 - 4. An important detail of these energy curves are the sharp avoided crossings at large R between the energy of the entrance channel (e.c.) and those of the states dissociating into N^{3+} + H^+ + H^+ in the limit $R \to \infty$. This sharpeness is due to the fact that at large R, the system has approximately $C_{\infty v}$ symmetry, and the avoided crossings between the energies of states of different approximate symmetry ($\Sigma - \Pi$, $\Sigma - \Delta$,...) are very narrow. In practice, the states involved in narrow crossings exhibit δ-function dynamical couplings between them, and the couplings of these states with the rest of the states change very rapidly in the avoided crossing region. Therefore, it is more convenient to employ a diabatized basis in the dynamical calculation, where the avoided crossings become crossings, as shown in figs. 2-4. The diabatic states have been constructed by applying a new technique to be published [27], which is based on the evaluation of the delayed overlap matrix elements:

$$S^*_{jk} =< \phi_j(R_i)|\phi_k(R_{i+1}) > \tag{6}$$

where R_i, R_{i+1} are two adjacent points of the grid of internuclear distances. When $|S^*_{j,j+1}|$ is larger than a given threshold value, we define a couple of diabatic states ϕ^d_j, ϕ^d_{j+1} whose energies cross between the points R_i and R_{i+1}. Besides, the sign of the delayed overlap allows us to ensure that the sign of each molecular wavefunction is the same in all grid points.

In figures 2- 4, the sizeable variation with ρ of the potential energy surfaces corresponding to the ADC states; they decay as $1/\rho$ as ρ increases because of the H^+-H^+ Coulomb interaction. This entails a variation in the position of the (avoided) crossings with the energy of the entrance channel (e.c.); in particular, the crossing between the e.c. curve and that of the $N^{3+}(3s^2)$ +H^++ H^+ takes place at $R \simeq 9.5$ a.u. for ρ=1.0a.u., at $R \simeq 6.5$ a.u. for ρ=1.4 a.u., and at $R \simeq 5.5$ a.u. for ρ=1.7a.u.; in the latter case the avoided crossing is wider and has not been diabatized. Similar effects can be noted for the energies of the other double capture channels. A consequence of this ρ dependence of the ADC potential energy surfaces, is that the identification of the SEC channels dissociating into $N^{4+}(1s^24l)$ + $H_2^+(1\sigma_g)$, which is relatively easy at short ρ (see fig. 2) becomes very difficult at ρ=1.7 (fig. 4) because their energies show many avoided crossings with that of the ADC channels. In

State	Present work	ref. [25]
$N^{4+}(1s^2\,3s)$	0	0
$N^{4+}(1s^2\,3p)$	0.0994	0.0989
$N^{4+}(1s^2\,3d)$	0.1320	0.1289
$N^{4+}(1s^2\,4s)$	0.6834	0.6842
$N^{4+}(1s^2\,4p)$	0.7241	0.7244
$N^{4+}(1s^2\,4d)$	0.7384	0.7369
$N^{4+}(1s^2\,4f)$	0.7410	—
$N^{5+}(1s^2)$	1.5172	1.5180
State	Present work	ref. [26]
$N^{3+}(1s^2\,3s^2)$	-1.2345	-1.2328
$N^{3+}(1s^2\,3s\,3p)$	-1.0986	-1.0834
$N^{3+}(1s^2\,3s\,3d)$	-1.0969	-1.0908

TABLE I: Calculated differences of the energies (in a.u.) of several atomic states with that of $N^{4+}(1s^2\,3s)$, compared with the spectroscopic values [25] for N^{4+} and N^{5+}, and accurate calculations [26] for the autonionizing states of N^{3+}.

practice, this makes very cumbersome to include molecular states correlating to $N^{4+}(4l)+ H_2^+$ in the dynamical calculation.

The main mechanism for SEC, indicated by the electronic energies of figs. 2-4, involves transitions from the entrance channel to the low-lying states correlating to $N^{4+}(3l)+ H_2^+(1\sigma_g)$ at R=4-5a.u., where the corresponding energies pseudocross. Since the crossings at large R are traversed diabaticaly, the main transitions to the ADC states take place at $R < 3.0$ a.u.. In the illustrations of figs. 2-4, we have also drawn the energy of the state that diabaticaly correlates to the dissociative single electron capture state $N^{4+}(3s)+ H_2^+(1\sigma_u)$; this shows avoided crossings with those of the ADC states, and furnishes a mechanism whereby they can be depopulated.

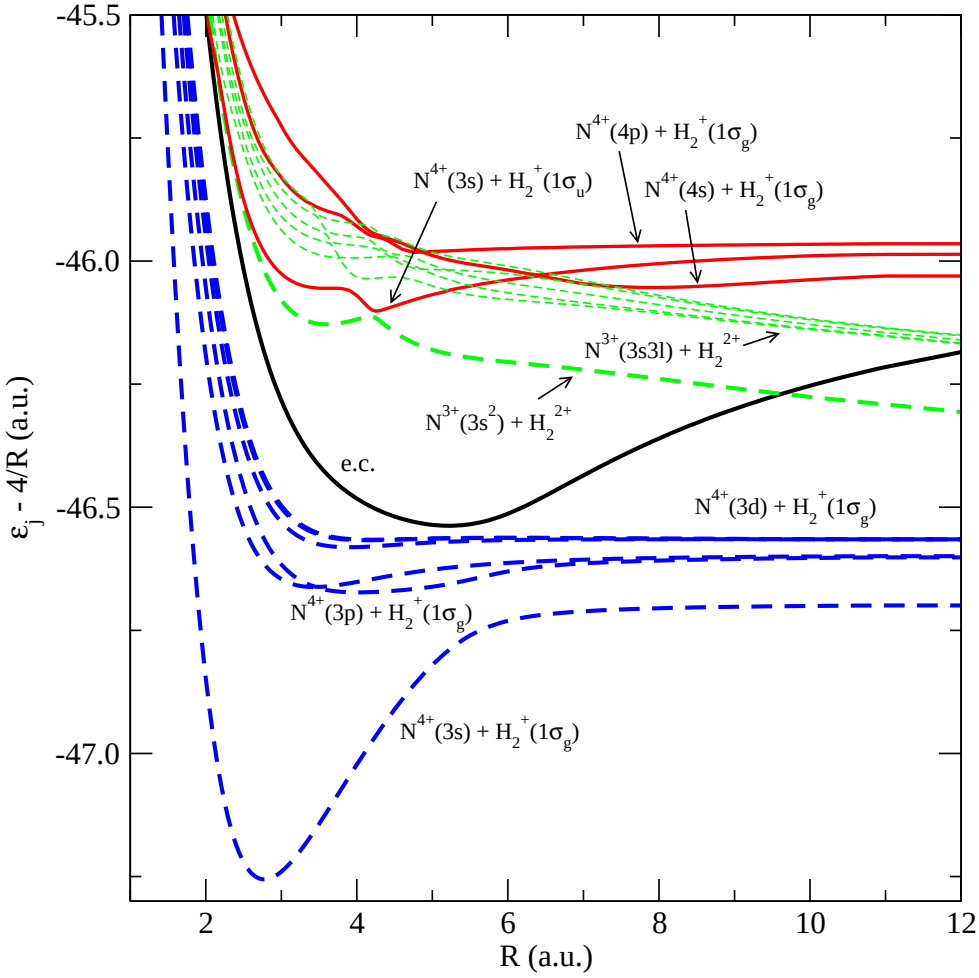

FIG. 2: Energies of the ^{1}A' electronic states of the NH_2^{5+} quasimolecule for ρ=1.0 a.u..

B. Dynamical method.

The method employed in our dynamical calculation has been explained in previous works of our group. Its main assumptions are:

1. The impact parameter method (see e.g. [17]), in which the position vector $\mathbf{R}$ of the incident ion with respect to the target molecule follows straight-line trajectories $\mathbf{R} = \boldsymbol{b} + \boldsymbol{v}t$ with constant velocity $\boldsymbol{v}$ and impact parameter $\boldsymbol{b}$. The remaining degrees of freedom are treated quantum mechanically, by means of the wavefunction $\Psi(\boldsymbol{r}, \boldsymbol{\rho}, t)$. Ψ is a solution of the equation:

$$\left(H_{\rm i} - {\rm i}\frac{\partial}{\partial t}\Big|_{\boldsymbol{r},\boldsymbol{\rho}} \right) \Psi(\boldsymbol{r}, \boldsymbol{\rho}, t) = 0 \qquad (7)$$

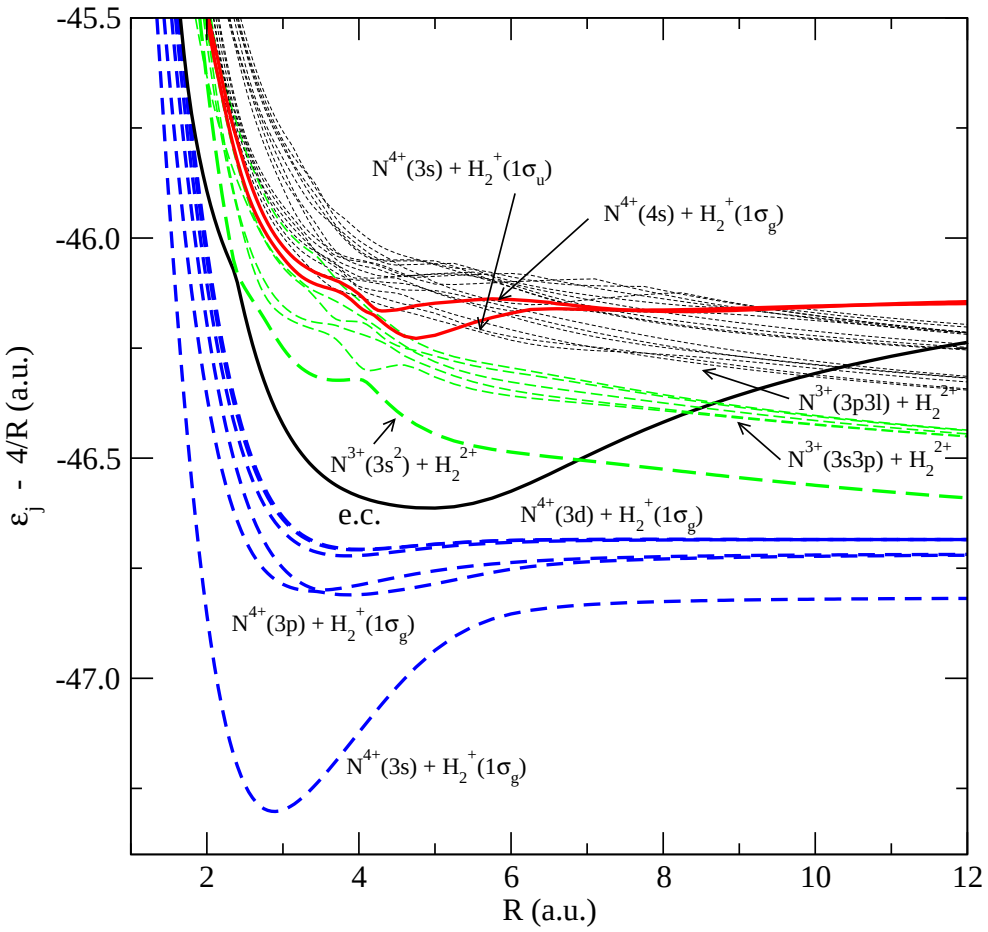

FIG. 3: Energies of the ^{1}A' electronic states of the NH_2^{5+} quasimolecule for ρ=1.4a.u..

with $\partial/\partial t = \boldsymbol{v}\cdot\nabla_R$,

$$H_{\rm i} = -\frac{1}{2\mu}\nabla_\rho^2 + H_{\rm elec}\ , \tag{8}$$

and $H_{\rm elec}$ is defined in (3).

2. A close-coupling expansion in terms of the molecular wavefunctions ϕ_j, which are approximate eigenfunctions of $H_{\rm elec}$ with energy ϵ_j.

3. The sudden approximation for rotation and vibration of the diatomic molecule, which assumes that the initial ro-vibrational wavefunction $\chi_0(\rho)Y_{JM}(\hat{\rho})$ does not appreciably change in the time interval in which the electronic transition takes place. One expands Ψ in the form:

$$\Psi(\boldsymbol{r},\boldsymbol{\rho},t) = \rho^{-1}Y_{JM}(\hat{\rho})\chi_0(\rho)\exp({\rm i}U)\sum_j a_j(t;\boldsymbol{\rho})\ \phi_j(\boldsymbol{r};\boldsymbol{\rho},\mathbf{R})\ \exp\left[-{\rm i}\int_0^t \epsilon_j {\rm d}t'\right] \tag{9}$$

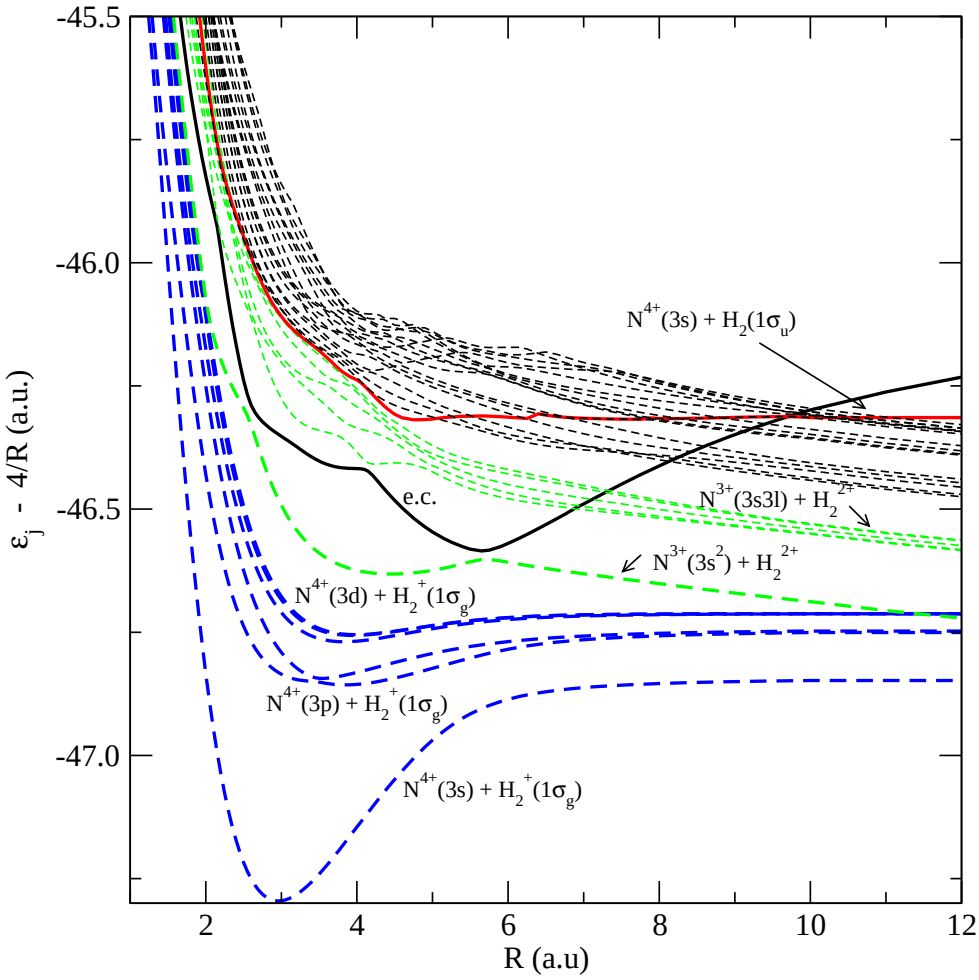

FIG. 4: Energies of the ^{1}A' electronic states of the NH_2^{5+} quasimolecule for ρ=1.7 a.u..

3bis When ρ is fixed at the equilibrium H-H distance ($\rho_0 \simeq 1.4$a.u. for H_2 ($X^1\Sigma_g^+$)) in the molecular wavefunctions of expansion (9), one obtains the familiar Franck-Condon (FC) approximation.

In the expansion (9), $\exp[\mathrm{i}U(\boldsymbol{r},t)]$ is a common translation factor (CTF) [28], and in the present calculation we have employed the CTF of ref. [29]. The expansion coefficients $a_j(t;\boldsymbol{\rho})$ are obtained by substituting expansion (9) in eq. (7). For fixed $\boldsymbol{rho}$, and for each nuclear trajectory these coefficients are the solutions of the system of differential equations:

$$\mathrm{i}\frac{\mathrm{d}a_j}{\mathrm{d}t} = \sum_k a_k \left\langle \phi_j \exp(\mathrm{i}U) \left| H_{\mathrm{elec}} - \mathrm{i}\left.\frac{\partial}{\partial t}\right|_{\boldsymbol{r},\boldsymbol{\rho}} \right| \phi_k \exp(\mathrm{i}U) \right\rangle \exp\left[-\mathrm{i}\int_0^t (\varepsilon_k - \varepsilon_j)\mathrm{d}t'\right] \quad (10)$$

The cross section for transition to a given electronic channel is [30]:

$$\sigma_f(v) = (4\pi)^{-1} \int \mathrm{d}\boldsymbol{b} \int \mathrm{d}\hat{\rho} \int \mathrm{d}\rho \chi_0^2 \left| a_f(\infty; \boldsymbol{\rho_0}) - \delta_{if} \right|^2 \tag{11}$$

The evaluation of the orientation averaged cross section of (11) requires to solve the system of differential equations (10) for several orientations of the vector $\boldsymbol{\rho}$ with respect to the nuclear velocity $\boldsymbol{v}$. Along the trajectory, the angle α between vectors $\boldsymbol{R}$ and $\boldsymbol{\rho}$ changes, which in practice requires the evaluation of the molecular wavefunctions ϕ_j in a grid of values of this angle, and the ensuing 2D interpolation of energies and couplings. A simplification of this procedure has been studied in previous works [30–32], where we have shown that a good approximation to the orientation averaged cross sections is given by an "isotropic" approximation, where the molecular wavefunctions of expansion (9) are assumed to vary little with α, and one employs the molecular data calculated for an intermediate value (between 45 ° and 60 °). In this work we have used this "isotropic" approximation with α = 60°. Explicitly:

$$\sigma_f(v) = 2\pi \int_0^\infty b P_f(b) \mathrm{d}b = \int_0^\infty \mathrm{d}\rho \chi_0^2 \int_0^\infty b \left| a_f(\infty; \rho, \alpha = 60^0) - \delta_{if} \right|^2 \mathrm{d}b \tag{12}$$

C. Dynamical couplings.

The transitions between the molecular states are induced by the non-adiabatic, or dynamical, couplings (see eq. (10)), which can be expressed as (see e.g. [18]):

$$\left\langle \phi_j \exp(\mathrm{i}U) \left| H_{\mathrm{elec}} - \mathrm{i}\frac{\partial}{\partial t} \right| \phi_k \exp(\mathrm{i}U) \right\rangle = \frac{v^2 t}{R} M_{ij} + \frac{bv}{R^2} R_{i,j} + \mathcal{O}(v^2) \tag{13}$$

The translation factor introduces terms proportional to v^2, which have been neglected in the present calculation. The terms proportional to v, M_{ij} and $R_{i,j}$, are respectively the modified radial and rotational couplings, which have the form:

$$M_{ij} = \left\langle \phi_i \left| \left. \frac{\partial \phi_j}{\partial R} \right|_{\alpha,\rho} \right\rangle + A_{ij}^R(R, \alpha, \rho) \tag{14}$$

and

$$R_{i,j} = \left\langle \phi_i \left| \left. \frac{\partial \phi_j}{\partial \alpha} \right|_{R,\rho} \right\rangle + A_{ij}^\alpha(R, \alpha, \rho) \ , \tag{15}$$

where $A_{ij}^{R,\,\alpha}$ are the corrections due to the common translation factor to first order in v.

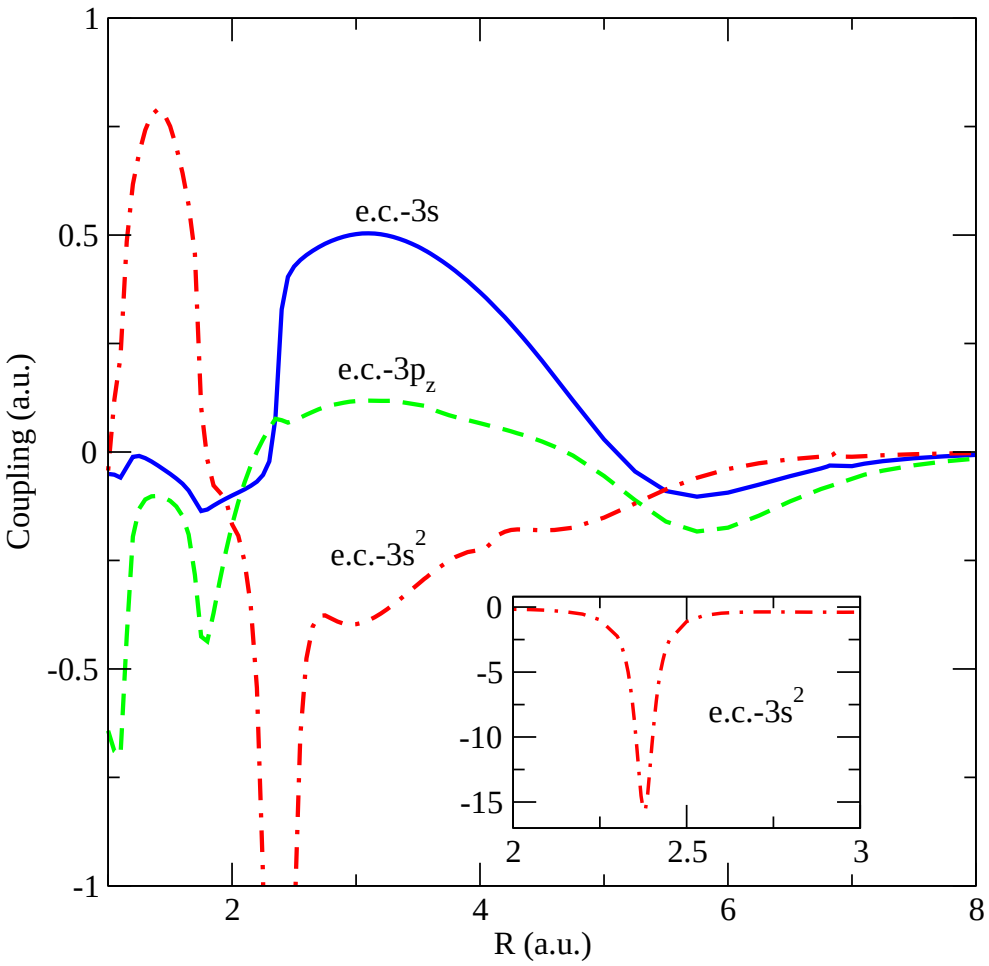

FIG. 5: Radial couplings between the entrance channel and the states correlating to N^4+(3s,3p)+ $H_2^+(1\ \sigma_g)$ and $N^{3+}(3s^2)$+ H^+ + H^+, for ρ=1.4 a.u. and α=60^0. The inset shows the peak of the coupling between the entrance channel and the state correlating to $N^{3+}(3s^2)$+ H^+ + H^+.

As an illustration, we show in fig. 5 the most important radial couplings (eq. (14)): for ρ = 1.4 a.u.. The main mechanism of the SEC reaction involves transitions from the entrance channel to the molecular states dissociating into N^{4+}(3s,3p)+ $H_2^+(1\sigma_g)$ in the wide avoided crossing at $R \simeq 4$ a.u., and where the corresponding radial couplings of fig. 5 show relative maxima. Transitions from the entrance channel to the state correlating to $N^{3+}(3s^2)$+ H^++H^+ are the main mechanism of the ADC process; these transitions take place in the neighborhood of the avoided crossing at $R \simeq 2.37$a.u., mainly induced by the tail of the radial coupling between these states. In turn, the rapid variation of the e.c. wavefunction in this region leads to the abrupt change of the radial couplings with the SEC states.

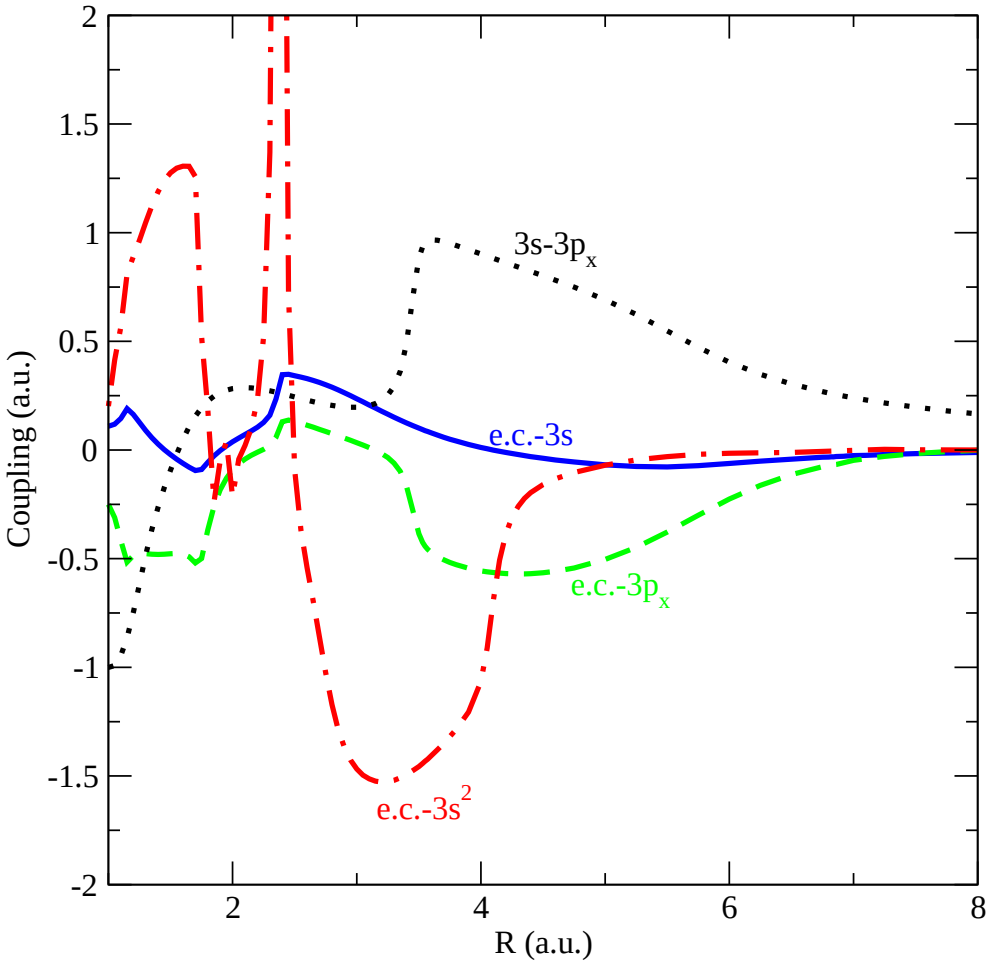

FIG. 6: Rotational couplings between the entrance channel and the states correlating to N^{4+}(3s,3p) + $H_2^+(1\ \sigma_g)$ and $N^{4+}(3s^2)$ + H^+ + H^+, for ρ=1.4 a.u. and α=60^o.

The structures of the most important rotational couplings (eq. (14)), shown in fig. 6, are related to the avoided crossings of fig. 3. In particular, the avoided crossing at $R \simeq$ 3.5a.u. between the energies of the states correlating to $N^{4+}(3p_x)+ H_2^+(1\sigma_g)$ and $N^{4+}(3p_z)+ H_2^+(1\sigma_g)$ yields the abrupt changes of the e.c.- $3p_x$ and 3s - $3p_x$ couplings. The e.c.-$3s^2$ avoided crossing at $R \simeq$ 2.37 a.u. leads to sharp peaks in both radial and rotational couplings. An avoided crossing at $R \simeq$ 2.00 a.u., between the energy curves of the entrance channel and the highest SEC state correlating to N^4+(3l)+ $H_2^+(1\sigma_g)$, which is difficult to notice in fig. 3, causes the changes of the e.c.- $3s^2$ and e.c. - $3p_x$ in this region.

III. RESULTS.

In a first step we have employed the FC approximation and a basis set that includes 17 states with the following correlations in the limit $R \to \infty$ (see fig. 3):

- The entrance channel that correlates to N^{5+}+ H_2 ($X^1\Sigma_g^+$).
- The 6 states that correlate to $N^{4+}(3l)$+ $H_2^+(1\sigma_g)$.
- Six states correlating to $N^{3+}(3s3l)$+ H^++H^+.
- One state correlating to $N^{4+}(3s)$+ $H_2^+(1\sigma_u)$.
- One state correlating to $N^{4+}(4s)$+ $H_2^+(1\sigma_g)$.
- The two lowest states correlating to $N^{3+}(3p3l)$+ H^++H^+

The total cross sections for single capture are plotted in fig. 7 together with the results of previous calculations at FC level and experimental results. Our cross sections for single electron capture show good agreement with the experimental data of Kearns *et al.* [5], and reasonable agreement with the photon emission experiments of refs. [3] and [4] for $E > 200$eV/amu. The usual IPM method is appropriate for $E \gtrsim 1.5$keV/amu, while the modification of ref. [15](called IPM-SEC in fig.7) extends this range down to $E \simeq 700$eV/amu. A good agreement at low E between the *ab initio* calculation and one-electron treatments [6, 7] without two-electron interpretation, was also found in [15, 21] for C^{4+}+ H_2 collisions, and it was explained there as due to a compensation of errors because the effective potentials were fitted to the experimental H_2 ionization potential instead of to the vertical one (for fixed ρ).

An illustration of the mechanism of SEC and ADC reactions is shown in figs. 8 and 9, where we have plotted the corresponding products $bP_k(b)$ obtained in the FC calculation. At low E (fig. 8), the calculation confirms the mechanism proposed in the previous section: the ADC process takes place at low b through transitions at R <3.0 a.u., induced by the e.c.-$3s^2$ radial coupling (see fig. 5), in the neighborhood of the avoided crossing between the corresponding energy curves. At these low energies, the main mechanism of the SEC reaction involves transitions at larger R ($\simeq$4.0 a.u.), where the couplings between the entrance channel and the states correlating to N^4+$(1s^23l)$ + $H_2^+(1\sigma_g)$ show relative maxima. On the other

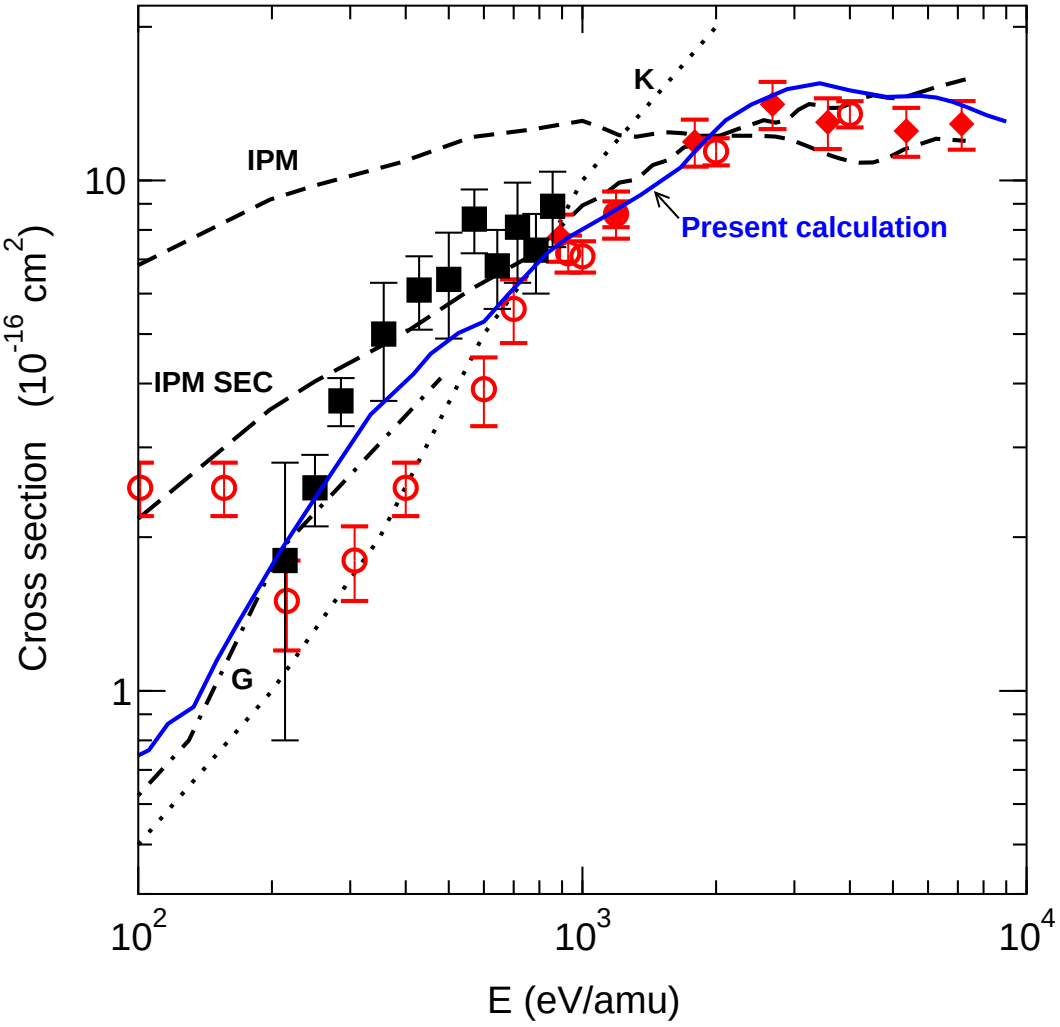

FIG. 7: Total cross sections for reaction (1): Calculations: —, present FC calculation; G, [6]; K, [7]; IPM, ref. [9]; IPM-SEC, ref. [16]. Experimental results: ♦; [3] ◯, [4]; ■, [5].

hand, the independent mechanisms of reactions (1) and (2), deduced from fig. 8, explains (see ref. [15]) the good agreement of the IPM-SEC results with the *ab initio* ones at $E \simeq$ 500 eV/amu.

At high energies, the avoided crossing at $R \simeq$2.37 a.u. is traversed diabatically, and the ADC transition probabilities do not show significant peaks at $b <$ 3a.u., as illustrated in fig. 9 for E=2keV/amu. The curves for SEC and ADC in figure 9 show maxima in the same regions of b, indicating that both reactions take place in the same regions of internuclear separations. Moreover, we have checked that the time evolution of the close-coupling coefficients suggests that ADC is now a two-step process through the SEC channels. At these energies, although

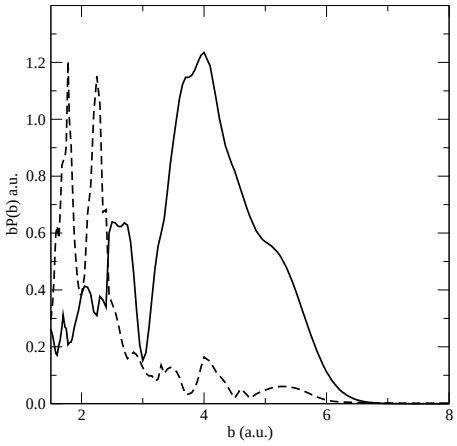

FIG. 8: Impact parameter times transition probabilities vs. b for SEC into N^{3+}(n=3) (full line) and ADC into N^{4+}(3s3l) (dashed line), calculated using the FC approximation and for an impact energy E= 500eV/a.m.u..

the mechanisms are not independent, the populations of the ADC channels are relatively small, and, accordingly, the SEC transition probabilities are not strongly modified by the transitions leading to ADC, thus explaining the reasonable agreement of IPM and IPM-SEC cross sections with the experimental ones in fig. 7. In this respect, a similar discussion has been recently presented in ref. [14] to explain the workings of the IPM approach for He^{2+} + H_2 collisions.

We have also carried out non FC dynamical calculations in the frame of the sudden approximation. We have checked that the cross sections of fig. 7 do not appreciably change when the two N^{3+}(3p3l) states and the state correlating to N^{4+}(4s)+ $H_2^+(1\sigma_g)$ are not included. Therefore, in these calculations we have employed a 14-state basis resulting of removing from the previous basis set these three states, which, as mentioned above, are difficult to include for ρ >1.4a.u.. Cross sections calculated within the vibrational sudden approximation for SEC into N^{4+}(3l) and ADC into N^{3+}(3s3l) are plotted in fig. 10, where they are compared with those from the FC calculation and the experimental ones. In general, relatively small changes are observed between the two calculations for SEC, while the comparison with the experimental values for ADC is slightly better for the sudden approximation calculation than for the FC ones.

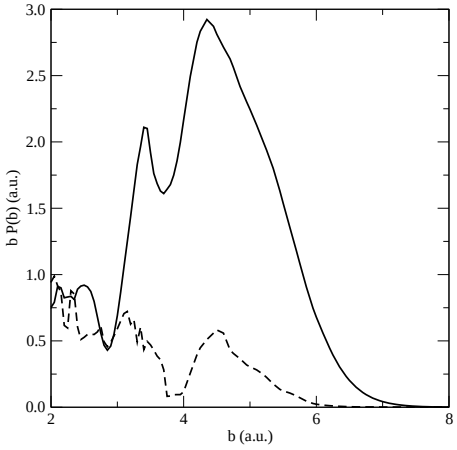

FIG. 9: Same as fig. 8 for E= 2keV/a.m.u..

A more stringent test of the calculations is provided by the comparison of the calculated partial cross sections for SEC with the photon emission measurements of refs. [3, 4]; this comparison is shown in fig 11, where we plot the ratios

$$\gamma_{\mathrm{s,\,p,\,d}} = \frac{\sigma_{\mathrm{s,\,p,\,d}}}{\sigma_3} \tag{16}$$

where σ_3 is the total cross section for formation of N^{4+}(n=3) in the SEC reaction, and $\sigma_{\mathrm{s,\,p,\,d}}$ are the partial cross sections for formation of N^{4+}(3s, 3p, 3d) in the same reaction, evaluated in the frame of the sudden approximation. Although we find general good agreement between experimental and calculated curves, some discrepancies can be noted both at low and high E, which are probably due to limitations of our calculation. In particular, at E >6keV/amu, the calculated population of N^{4+}(3p) is larger than that of N^{4+}(3d), which can be due to the lack of N^{4+}(n=4)+ H_2^+ channels. At E <200eV/amu, the increase of the experimental total cross section in fig. 10 is probably a consequence of transitions between vibronic states, which are not accurately taken into account by the vibrational sudden approximation; this can also cause of the already mentioned differences between theory and experiment for total cross sections at low E (fig. 10).

IV. CONCLUSIONS

We have presented the first *ab initio* calculation of SEC and ADC cross sections in collisions of N^{5+}ions with H_2at impact energies between 0.1 and 10 keV/amu, by applying

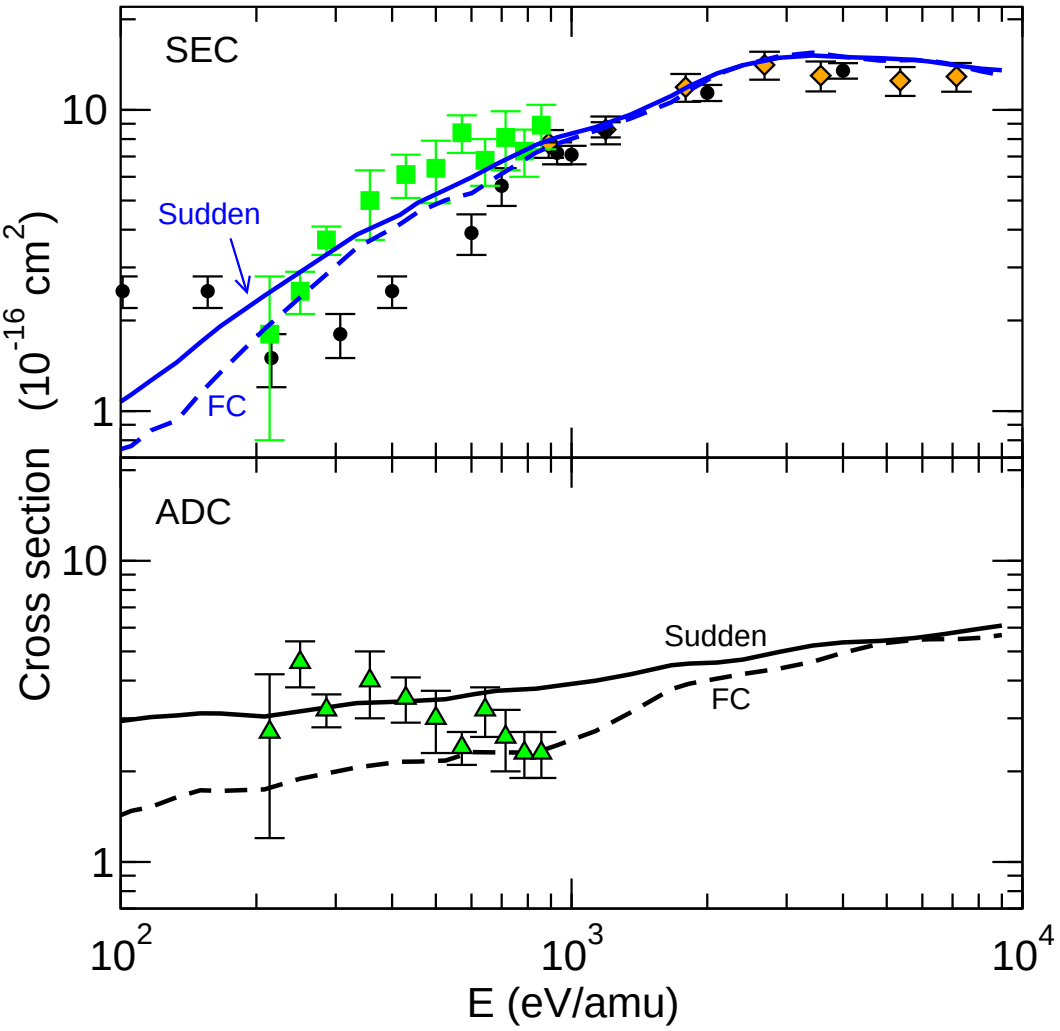

FIG. 10: Total cross sections for SEC (1) and ADC (2) reaction: Lines: present calculations, employing the sudden and FC approximations as indicated in the figure. Experimental results for SEC: ⋄; [3] ∘,ref. [4]; ■, [5]. Experimental cross sections for ADC:, present calculation; ▲, [5]

the sudden approximation for vibration and rotation of the diatomic molecules. The energy range where our calculation is accurate is limited by the approximations employed. At low energies (E <100eV/amu), the sudden approximation for vibration probably causes the discrepancy with photon emission measurements [4] between 100 and 200 eV/amu. At higher energies, the main limitation of our treatment is the truncation of the molecular basis set, and in particular, the lack of states correlating to $N^{4+}(4l) + H_2^+(1\sigma_g)$ in that basis. Although we obtain good agreement with the experimental total SEC cross sections at $E \simeq$ 10keV/amu, the truncation of the basis set limits the validity of our calculation of SEC

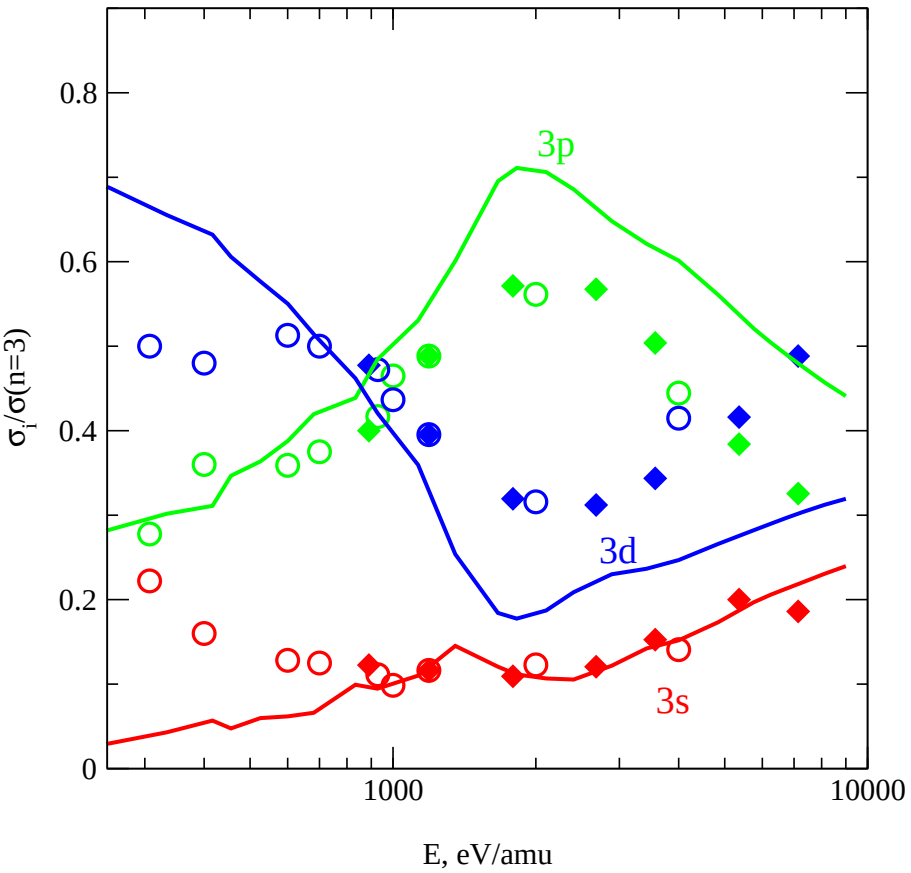

FIG. 11: Ratios $\sigma(3l)/\sigma(n=3)$ of the partial cross sections for population of $N^4(n=3)$ levels in reaction (1). Lines, present results. Experimental results: ◯, [3]; ♦, ref. [4]

partial cross section to E <5keV/amu.

With respect to the comparison with previous calculations that used the IPM approach, our cross section for SEC agrees with the IPM values for E >2keV/amu, and the agreement extends to E >700 eV/amu for the IPM-SEC method of ref. [15]. Our results also show good agreement with the recent experimental data of [5] in the energy range 0.2≤ E ≤1keV/amu for SEC into N^{4+}(n=3) and ADC. We have also found good agreement with the data of refs. [3] and [4] for the branching ratio of 3s, 3p and 3d levels of N^{4+} formed in the SEC reaction, in the energy range 0.2≤ E ≤6keV/amu.

Acknowledgments

This work has been partially supported by DGICYT projects BFM2000-0025 and FTN2000-0911.

---

[1] T. E. Cravens, Science **296**, 1042 (2002).

[2] R. Janev, Atomic and Plasma-Material Interaction Data for Fusion **9**, 1 (2001).

[3] D. Dijkkamp, D. Ciric, E. Vlieg, A. de Boer, and J. de Heer, J. Phys. B: At. Mol. Opt. Phys. **18**, 4763 (1985).

[4] G. Lubinski, Z. Juhász, R. Morgenstern, and R. Hoekstra, J. Phys. B: At. Mol. Opt. Phys. **33**, 5275 (2000).

[5] D. M. Kearns, R. W. McCullough, and H. B. Gilbody, J. Phys. B: At. Mol. Opt. Phys. **35**, 4335 (2002).

[6] M. Gargaud and R. McCarroll, J. Phys. B: At. Mol. Phys. **18**, 463 (1985).

[7] A. Kumar and B. C. Saha, Phys. Rev. A **59**, 1273 (1999).

[8] D. Elizaga, L. F. Errea, J. D. Gorfinkiel, L. Méndez, A. Macías, A. Riera, A. Rojas, O. J. Kroneisen, T. Kirchner, H. J. Lüdde, et al., J. Phys. B: At. Mol. Opt. Phys. **32**, 857 (1999).

[9] D. Elizaga, L. F. Errea, A. Macías, L. Méndez, A. Riera, and A. Rojas, Phys. Scr. **T80**, 187 (1999).

[10] J. H. McGuire and L. Weaver, Phys. Rev. A **16**, 41 (1977).

[11] V. Sidorovich, J. Phys. B: At. Mol. Phys. **14**, 4805 (1981).

[12] H. J. Lüdde and R. M. Dreizler, J. Phys. B: At. Mol. Opt. Phys. **18**, 107 (1985).

[13] A. L. Godunov, J. H. McGuire, P. B. Ivanov, V. A. Shipakov, H. Merabet, R. Bruch, J. Hanni, and K. K. Shakov, J. Phys. B: At. Mol. Opt. Phys. **34**, 5055 (2001).

[14] L. F. Errea, A. Macias, L. Méndez, B. Pons, and A. Riera, J. Phys. B: At. Mol. Opt. Phys. p. in press (2003).

[15] L. Errea, J. D. Gorfinkiel, C. Harel, H. Jouin, A. Macías, L. Méndez, B. Pons, and A. Riera, J. Phys. B: At. Mol. Opt. Phys. **33**, 3107 (2000).

[16] L. F. Errea, A. Macías, L. Méndez, I. Rabadán, A. Riera, and P. Sanz, Int. J. Quant. Chem. **86**, 182 (2002).

[17] B. H. Bransden and M. H. C. McDowell, *Charge Exchange and the Theory of Ion-Atom Collisions* ((Oxford: Clarendon), 1992).

[18] L. F. Errea, A. Macias, L. Méndez, B. Pons, and A. Riera, J. Chem. Phys. p. in press (2003).

[19] L. Pichi, Y. Li, H. L. R. J. Buenker, and M. Kimura, J. Chem. Phys. **118**, 4872 (2003).

[20] L. F. Errea, J. D. Gorfinkiel, E. S. Kryachko, A. Macías, L. Méndez, and A. Riera, J. Chem. Phys. **106**, 172 (1997).

[21] L. F. Errea, J. D. Gorfinkiel, A. Macías, L. Méndez, and A. Riera, J. Phys. B: At. Mol. Opt. Phys. **32**, 1705 (1999).

[22] A. Macías and A. Riera, Phys. Rep. **81**, 299 (1982).

[23] E. Davidson, in *MOTECC, Modern Techniques in Computational Chemistry*, edited by E. Clementi (ESCOM Publishers B. V., Leiden, 1990).

[24] V. López, A. Macías, R. D. Piacentini, A. Riera, and M. Yáñez, J. Phys. B: At. Mol. Phys. **11**, 2889 (1978).

[25] C. E. Moore, *Atomic Energy Levels Nat. Stand. Ref. Data Series vol. 1* ((US National Bureau of Standards), 1971).

[26] H. Bachau, P. Galan, F. Martín, A. Riera, and M. Yáñez, At. Data. Nucl. Data Tables **44**, 305 (1990).

[27] L. F. Errea, L. Fernández, A. Macías, L. Méndez, I. Rabadán, and A. Riera, J. Chem. Phys. p. To be submited (2003).

[28] S. B. Schneiderman and A. Russek, Phys. Rev. **181**, 311 (1969).

[29] L. F. Errea, L. Méndez, and A. Riera, J. Phys. B: At. Mol. Opt. Phys. **15**, 101 (1982).

[30] L. F. Errea, J. D. Gorfinkiel, A. Macías, L. Méndez, and A. Riera, J. Phys. B: At. Mol. Opt. Phys. **30**, 3855 (1997).

[31] L. F. Errea, A. Macías, L. Méndez, and A. Riera, J. Phys. B: At. Mol. Opt. Phys. **32**, 4065 (1999).

[32] L. F. Errea, A. Macías, L. Méndez, I. Rabadán, and A. Riera, Int. J. Mol. Sci. **3**, 142 (2002).

[33] The basis set is available from the authors upon request